ELECTRONIC SUPPORTING INFORMATION FILE

O_2 Reduction via Proton-Coupled Electron Transfer by a V(III) Aquo on a Polyoxovanadate-alkoxide Cluster.

Shannon E. Cooney[ϕ], Eric Schreiber[ϕ], Baela M. Ferrigno, Ellen M. Matson*

Department of Chemistry, University of Rochester, Rochester, New York 14627, USA

[ϕ]Authors contributed equally to this work.

Supporting Information Table of Contents

General Considerations. All manipulations were carried out in the absence of water and oxygen using standard Schlenk techniques or in a UniLab MBraun inert atmosphere drybox under a dinitrogen atmosphere. All glassware was oven dried for a minimum of 4 h and cooled in an evacuated antechamber prior to use in the drybox. Solvents were dried and deoxygenated on a glass contour system (Pure Process Technology, LLC) and stored over 4 Å molecular sieves purchased from Fisher Scientific and activated prior to use. **1-$[V_6O_7(OCH_3)_{12}]^{1-}$**, and 5,10-dihydrophenazine (H_2Phen), 5,10-dihydrophenazine-d_2 (D_2Phen) were synthesized according to literature precedent.[1-3] TEMPO was purchased from Sigma-Aldrich and used as received.

^{1}H NMR spectra were recorded at 500 MHz on a Bruker DPX-500 MHz spectrometer locked on the signal of deuterated solvents. All chemical shifts were reported relative to the peak of residual H signal in deuterated solvents. THF-d_8 and MeCN-d_3 were purchased from Cambridge Isotope Laboratories and stored in the drybox over activated 4 Å molecular sieves. Infrared (FT-IR, ATR) spectra of complexes were recorded on a Perkin Elmer Spectrum 3 Fourier Transform Infrared Spectrophotometer and are reported in wavenumbers (cm^{-1}). Electronic absorption measurements were recorded at room temperature in anhydrous THF in a sealed 1 cm quartz cuvette with an Agilent Cary 60 UV-Vis spectrophotometer or an Agilent Cary 3500 spectrophotometer. Kinetic experiments were carried out on an Agilient Cary 3500 UVVis spectrophotometer with an integrated Peltier temperature control system.

Synthesis of $[(CH_3(CH_2)_7)_2N][V_6O_6(OH_2)(OCH_3)_{12}]$ ***2-$V_6O_6(OH_2)^{1-}$***. In a glovebox, a 20 mL scintillation vial was charged with ***1-$V_6O_7^{1-}$*** (0.217 g, 0.173 mmol) and 10 mL of THF. H_2Phen (0.035 g, 0.190 mM) was added as a solid with stirring overnight (16 hr) to ensure completion. After ~2 hr, the solution turned from green to maroon. Volatiles were removed *in vacuo*, and the resulting crude solid was washed with 3:1:0.5 pentane / diethyl ether / THF mixture (3 x 10 mL) and filtered over celite (1 cm). Minimal THF in the washing mixture aids in removing any unreacted H_2Phen. The solid was extracted in THF to yield ***2-$V_6O_6(OH_2)^{1-}$***(0.128 g, 0.101 mmol, 59%). ^{1}H NMR (500 MHz, THF-d_8) δ = 26.04, 3.52, 1.31, 0.90, and −14.90 ppm. UV-Vis/NIR (THF, 21 °C) λ = 418 nm (ε = 875 M^{-1} cm^{-1}), 519 nm (ε = 1137 M^{-1} cm^{-1}), 636 nm (ε = 586 M^{-1} cm^{-1}), 1010 nm (ε = 138 $M^{-1}cm^{-1}$). IR (ATR) O-H = 3429 cm^{-1}, C-H = 3000-2800, V-OMe = 1042 cm^{-1}, V=O = 953 cm^{-1}. Elemental analysis was not determined for ***2-$V_6O_6(OH_2)^{1-}$***, as the molecular weight of the parent cluster (***1-$V_6O_7^{1-}$***, 1257 g mol^{-1}) and the daughter cluster (***2-$V_6O_6(OH_2)^{1-}$,*** 1259 g mol^{-1}) vary only by two atomic units. Variation between these two molecular weights is well within the error of the instrument (± 0.4 %), ***1-$V_6O_7^{1-}$*** calculated; C: 42.0%, H: 8.4%, N: 1.1%, ***2-$V_6O_6(OH_2)^{1-}$*** calculated 41.9%, H: 8.5%, N: 1.1%.[4] Evidence of successful removal of organic reagents was observed by ^{1}H NMR.

Synthesis of $[(CH_3(CH_2)_7)_2N][V_6O_7(OCH_3)_{12}]$ ***1-$V_6O_7^{1-}$*** *by TEMPO reduction.* In a glovebox, a 20 mL scintillation vial was charged with ***2-$V_6O_6(OH_2)^{1-}$*** (0.003 g, 0.002 mmol), 0.2 mL of a 110 mM stock solution of TEMPO in THF, and 5 mL of THF. The mixture was stirred for 3 hours to ensure completion. After ~2, the solution turned from maroon to green. Volatiles were removed *in vacuo*, the product TEMPO-H sublimes and can be removed by vacuum. The remaining solid was identified as ***1-$V_6O_7^{1-}$*** (0.003 g, 0.002 mmol, >99 %) and matched the previously reported ^{1}H NMR spectrum.[1]

Synthesis of $[(CH_3(CH_2)_7)_2N][V_6O_7(OCH_3)_{12}]$ ***1-$V_6O_7^{1-}$*** *by O_2 reduction.* In a glovebox, a 50 mL round bottom was charged with ***2-$V_6O_6(OH_2)^{1-}$*** (0.023 g, 0.018 mmol) and 10 mL of THF. The round bottom was sealed with a septum and removed from the glovebox. Anhydrous O_2 was bubbled through the mixture with an outlet needle and was stirred for 2 hours to ensure completion. After ~2 hr, the solution turned from maroon to green. Volatiles were removed *in vacuo*. The solid was identified as ***1-$V_6O_7^{1-}$*** (0.011 g, 0.009 mmol, 50%) and matched the previously reported ^{1}H NMR spectrum.[1]

Synthesis of $[(CH_3(CH_2)_7)_2N][V_6O_6(OD_2)(OCH_3)_{12}]$ ***2-$V_6O_6(OD_2)^{1-}$***. In a glovebox, a 20 mL scintillation vial was charged with ***1-$V_6O_7^{1-}$*** (0.158 g, 0.125 mmol) and 10 mL of THF. D_2Phen (0.025 g, 0.138 mmol)

was added as a solid with stirring overnight (16 hr) ensure completion. After ~4 hr, the solution turned from green to maroon. Volatiles were removed *in vacuo*, and the resulting crude solid was washed with 3:1:0.5 pentane / diethyl ether / THF mixture (3 x 10 mL) and filtered over celite (1 cm). Minimal THF in the washing mixture aids in removing any unreacted D_2Phen. The solid was extracted in THF to yield ***2-V$_6$O$_6$(OD$_2$)$^{1-}$*** (0.149 g, 0.119 mmol, 94%). ^{1}H NMR (500 MHz, THF-d_8) δ = 25.80, 3.22, 1.31, 0.89, and −14.43 ppm. IR (ATR) C-H = 3000-2800 (O-H stretch may be obstructed by these bands, V-OMe = 1050 cm^{-1}, V=O = 947 cm^{-1}. UV-Vis/NIR (THF, 21 °C) λ = 445 nm (ε = 1063 M^{-1} cm^{-1}), 510 nm (ε = 1236 M^{-1} cm^{-1}), 620 nm (ε = 725 M^{-1} cm^{-1}), 999 nm (ε = 165 M^{-1} cm^{-1}). Elemental analysis was not determined for ***2-V$_6$O$_6$(OD$_2$)$^{1-}$***, as the molecular weight of the parent cluster (***1-V$_6$O$_7^{1-}$***, 1257 g mol^{-1}) and the daughter cluster (***2-V$_6$O$_6$(OD$_2$)$^{1-}$,*** 1259 g mol^{-1}) vary only by four atomic units. Variation between these two molecular weights is well within the error of the instrument (± 0.4 %), ***1-V$_6$O$_7^{1-}$*** calculated; C: 42.0%, H: 8.4%, N: 1.1%, ***2-V$_6$O$_6$(OD$_2$)$^{1-}$*** calculated 41.9%, H: 8.7%, N: 1.1%.[4] Evidence of successful removal of organic reagents was observed by ^{1}H NMR.

Determining Order with Respect to TEMPO for the oxidation of 2-V$_6$O$_6$(OH$_2$)$^{1-}$: Pseudo-first-order reaction conditions were used to establish the rate expression for the reaction between **2-V$_6$O$_6$(OH$_2$)$^{1-}$** and TEMPO were tracked by monitoring the absorbance at 1025 nm over the reaction coordinate. Final TEMPO concentrations were varied from 5 to 45 mM, with a constant concentration of 0.30 mM **2-V$_6$O$_6$(OH$_2$)$^{1-}$**. Samples of cluster stock solutions in THF were loaded in a long-necked quartz cuvette and sealed with a rubber septum and electrical tape before removing from the glovebox. In a 1 mL syringe, a sample of oxidant stock solution (~160 mM in THF) was measured inside the glovebox. After equilibrating to 25 °C in the spectrophotometer, data acquisition began, and the reductant solution was forcefully injected to ensure efficient sample mixing. Upon the conclusion of the reaction, the initial rate was obtained by linear fitting of the reaction from 0 – 15 % completion, where the initial rate is the slope of the linear fit.[5] Percent completion is calculated by determining the expected change in absorbance between the reactant and product clusters. Plotting the initial rates as a function of TEMPO results in a linear relationship, where the experimentally derived rate constant (k_{exp}) is equal to the slope. (Figure S7-S10).

General procedure for determining activation parameters for the oxidation of 2-V$_6$O$_6$(OH$_2$)$^{1-}$ by TEMPO: Eyring analysis was performed by collecting absorbance *vs.* time data at temperatures between 0 and 25 °C. Reactions were assembled in an analogous fashion to previously run experiments, with constant oxidant and cluster concentrations of 10.0 and 0.30 mM, run in triplicate (Fig. S11). Conversion of k_{obs} to k_{exp} was done by dividing k_{obs} by the initial oxidant concentration (10 mM). Plotting ln(k_{exp}/T) as a function of $1/T$ (temperature converted in K), the linear plot was used to solve for activation parameters using the below equations where R is the gas constant in units of cal (mol^{-1} K^{-1}), k_{Boltz} is Boltzmann's constant, and h_{Planck} is Planck's constant, m is the slope, and b is the y-intercept.

$$ln\frac{k_{exp}}{T} = m \times \frac{1}{T} + b$$

$$\Delta H^{\ddagger} = m \times -R$$

$$\Delta S^{\ddagger} = R \times [b - ln\frac{k_{Boltz}}{h_{Planck}}]$$

$$\Delta G^{\ddagger} = \Delta H^{\ddagger} - T\Delta S^{\ddagger}$$

Preparation of O_2 Stock Solution for Kinetic Experiments: In a drybox, a 100 mL round bottom flask with molecular sieves was charged with 50 mL anhydrous degassed THF and sealed with a rubber septum and electrical tape. The flask was removed from the drybox and was then placed in a water bath set to 25 °C. The THF was sparged with anhydrous O_2 for at least 30 min by first passing the gas through a drying

column filled with activated Drierite. The resulting solution was saturated with O_2 to a concentration of 10.1 mM.[6]

Determining Order with Respect to 2-$V_6O_6(OH_2)^{1-}$: Pseudo-first-order reaction conditions were used to establish the rate expression for the reaction between **2-$V_6O_6(OH_2)^{1-}$** the and 3.0 mM O_2 were tracked by monitoring the absorbance at 1025 nm over the reaction coordinate. Final **2-$V_6O_6(OH_2)^{1-}$** concentrations were varied from 0.10 to 0.25 mM, with a constant concentration of O_2 of 3.0 mM. Samples of cluster stock solutions in THF were loaded in a long-necked quartz cuvette and sealed with a rubber septum and electrical tape before removing from the glovebox. In a 1 mL syringe, a sample of oxidant stock solution (10.1 mM in THF) was measured outside of the glovebox and injected into the cuvettes. After equilibrating to 25 °C in the spectrophotometer, data acquisition began, and the cluster solution was forcefully injected to ensure efficient sample mixing. Upon the conclusion of the reaction, the initial rate was obtained by linear fitting of the reaction from 5 – 15 % completion, where the initial rate is the slope of the linear fit.[5, 7] A log-log plot of initial rates and [**2-$V_6O_6(OH_2)^{1-}$**] similarly reveal a first order dependence on **2-$V_6O_6(OH_2)^{1-}$**, with a slope equal to ~1 (Figure S18 – S20).

Determining Order with Respect to O_2: Pseudo-first-order reaction conditions were used to establish the rate expression for the reaction between **2-$V_6O_6(OH_2)^{1-}$** the excess O_2 (10 – 27 equivalents) were tracked by monitoring the absorbance at 1025 nm over the reaction coordinate. Final oxidant concentrations were varied from 3.0 to 7.7 mM, with a constant concentration of cluster of 0.30 mM. Samples of THF and cluster were loaded in a long-necked quartz cuvette and sealed with a rubber septum before removing from the glovebox. In a 1 mL syringe, a sample of oxidant stock solution (10.1 mM in THF), was measured outside of the glovebox. After equilibrating to 25 °C in the spectrophotometer, data acquisition began, and the oxidant solution was forcefully injected to ensure efficient sample mixing. Upon the conclusion of the reaction, the initial rate was obtained by linear fitting of the reaction from 5 – 15 % completion, where the initial rate is the slope of the linear fit. A log-log plot of initial rates and [O_2] similarly reveal a first order dependence on O_2, with a slope equal to ~1 (Figure S21).[5, 7]

Uncertainties were determined by performing a linear regression function on data from triplicate trials for each condition in Microsoft Excel and calculating a 95% confidence interval. The reported errors are the first significant figure of the difference between the determined slope and the confidence interval maximum.

Determining the Rate of Reactions for 2-$V_6O_6(OH_2)^{1-}$ and $[(V_6O_7(OH)_6(TRIS^{NO2})_2]^{2-}$. The pseudo-first order rate expressions for ORR by **2-$V_6O_6(OH_2)^{1-}$** (k_{obs} = 0.04 M^{-1} s^{-1}) and $[(V_6O_7(OH)_6(TRIS^{NO2})_2]^{2-}$ (k_{obs} = 9.6 x 10 $M^{-0.5}$ s^{-1}) are used to calculate the rate at 10 mM O_2 using the following equations:

$$Rate_{V_6O_7(OH)_6(TRIS^{NO2})_2} = k_{obs}[O_2]^{-0.5}$$

$$Rate_{V_6O_6(OH_2)} = k_{obs}[O_2]^1$$

The rate determining step of ORR from **2-$V_6O_6(OH_2)^{1-}$** and $[(V_6O_7(OH)_6(TRIS^{NO2})_2]^{2-}$ are both established to be $1H^+/1e^-$ process, so a probability factor (n) is introduced to normalize the two rates ($Rate_{normalized}$) to account for the number of H^+/e^- pairs on the surface of the cluster. For **2-$V_6O_6(OH_2)^{1-}$** n = 2, and $[(V_6O_7(OH)_6(TRIS^{NO2})_2]^{2-}$ n = 6.

$$Rate_{normalized} = \frac{Rate}{n}$$

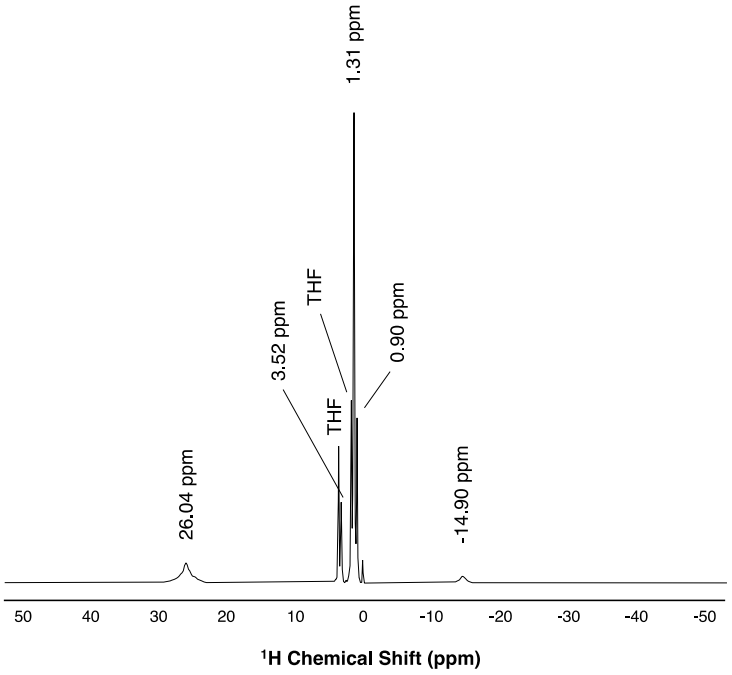

Figure S1. ^{1}H NMR of **2-$V_6O_6(OH_2)^{1-}$** in THF-d_8, 21 °C.

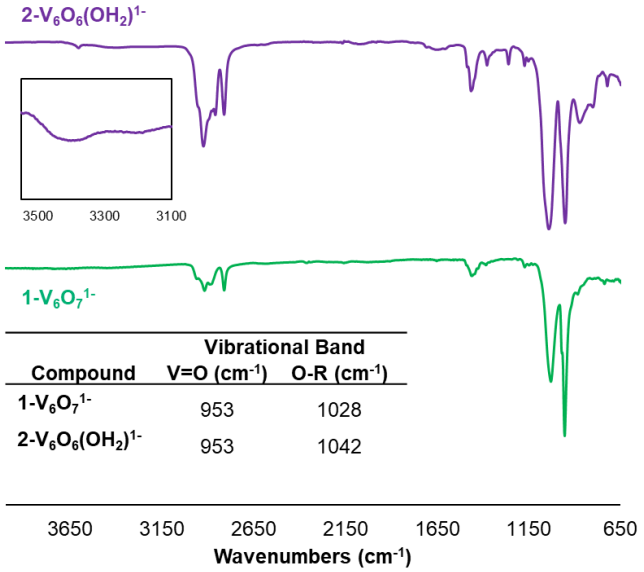

Figure S2. IR Spectra of **1-$V_6O_7^{1-}$** (green) and **2-$V_6O_6(OH_2)^{1-}$** (purple), neat 21 °C. A small broad band at 3429 cm^{-1} is attributed to the O-H bond stretching frequency of the V-OH_2.

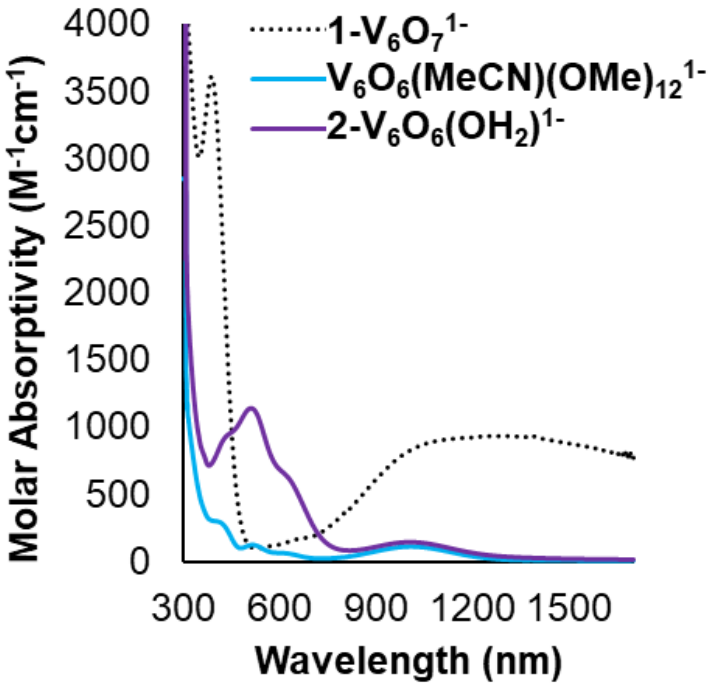

Figure S3. EAS of **1-$V_6O_7^{1-}$** (black dotted trace), **2-$V_6O_6(OH_2)^{1-}$** (purple trace), and $V_6O_6(MeCN)(OMe)_{12}^{1-}$ (blue trace) in THF, 21 °C.

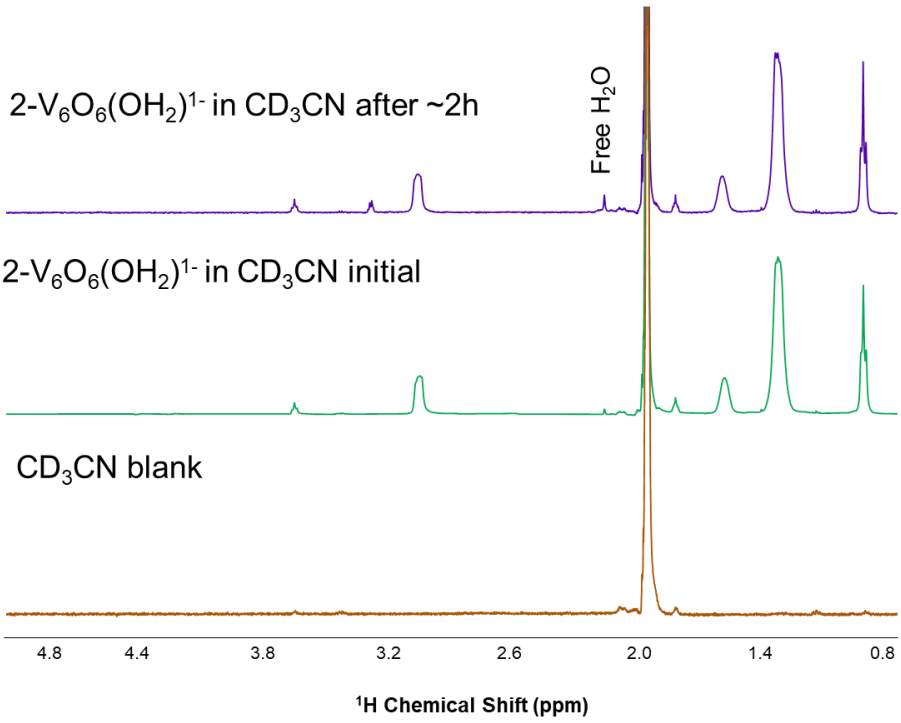

Figure S4. Diamagnetic ^{1}H NMR of **2-$V_6O_6(OH_2)^{1-}$** in CD_3CN to show the dissociation of the OH_2 over time.

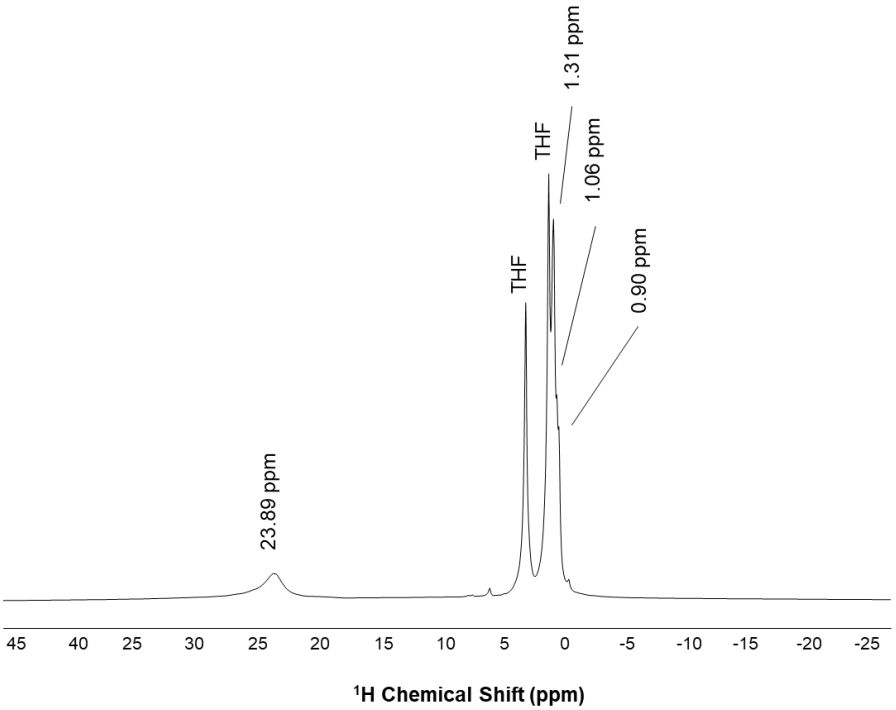

Figure S5. **2-$V_6O_6(OH_2)^{1-}$** + 2 eq of TEMPO in THF-d_8.

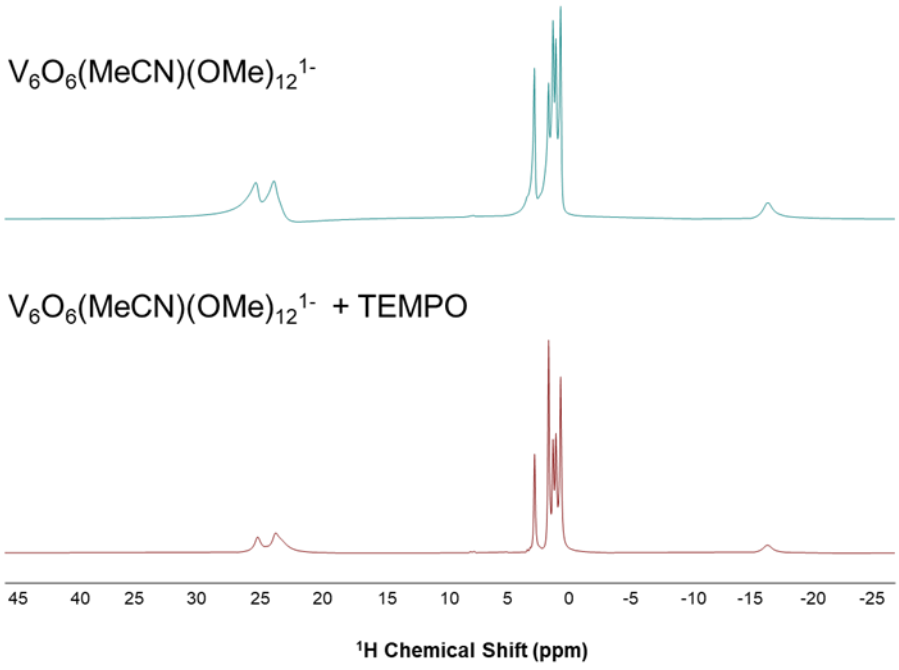

Figure S6. $V_6O_6(MeCN)^{1-}$ + XS TEMPO in CD_3CN showing no conversion to $V_6O_7^{1-}$, suggesting in the MeCN bond assembly there are no reactive H•.

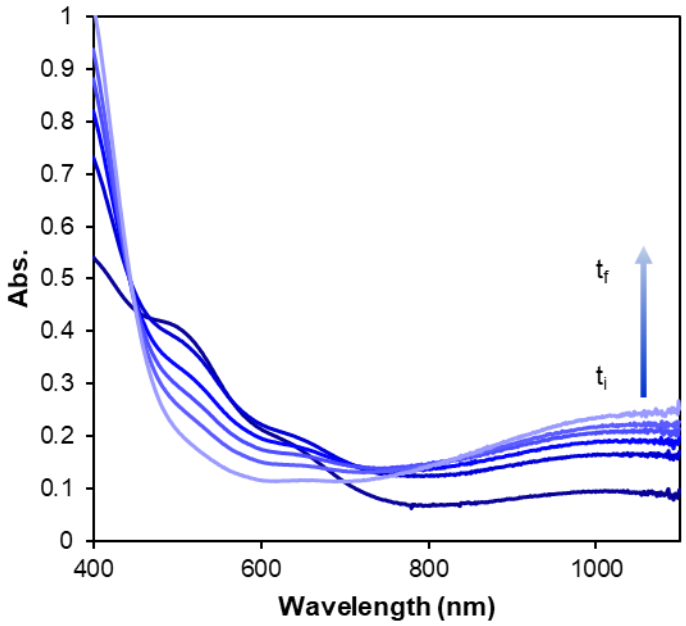

Figure S7. EAS Scanning kinetics at of 0.30 mM **2-$V_6O_6(OH_2)^{1-}$** + 10 mM TEMPO in THF, 25 °C. t_f = ~ 1 hr.

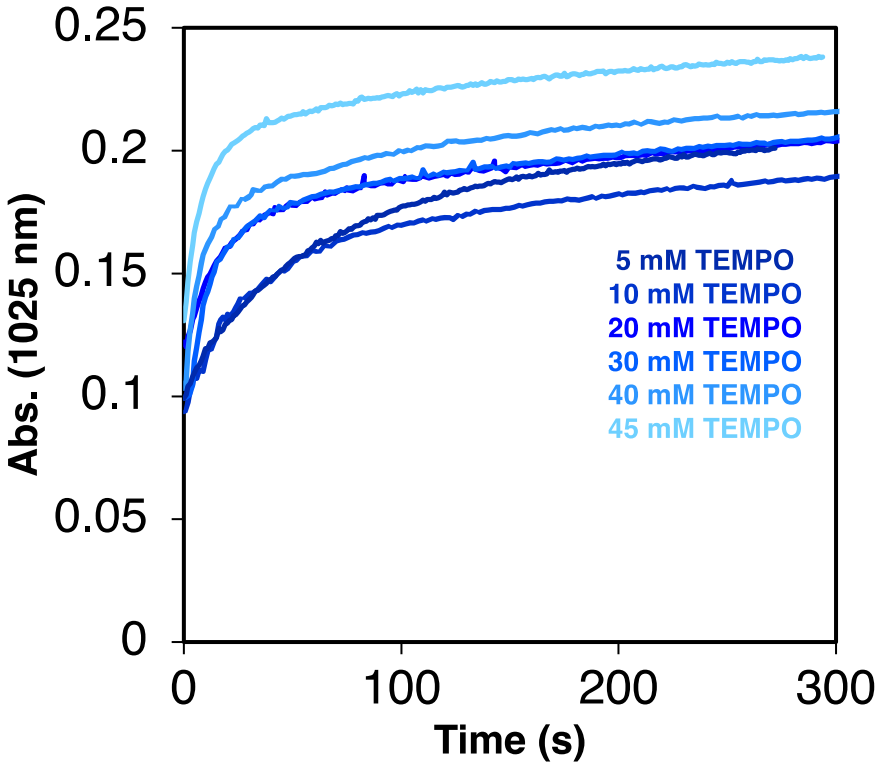

Figure S8. EAS Kinetics traces at 1025 nm of 0.30 mM **2-$V_6O_6(OH_2)^{1-}$** + excess ((5 – 45 mM) TEMPO in THF, 25 °C.

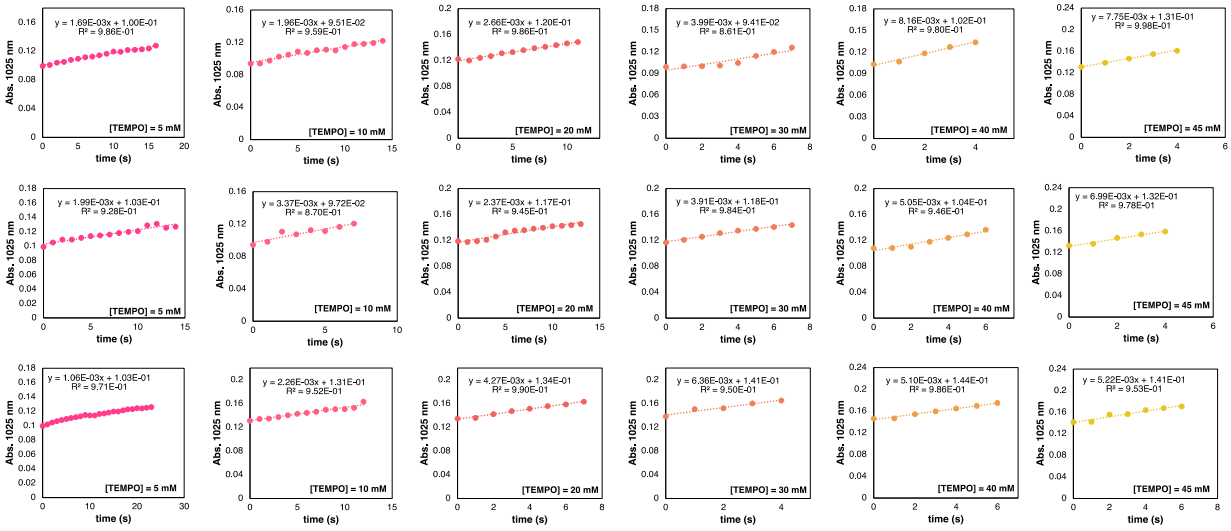

Figure S9. Kinetic traces at 1025 nm of 0.30 mM **2-$V_6O_6(OH_2)^{1-}$** + varied concentration of TEMPO in THF, 25 °C. Traces are fit from 0 – 15 % completion of the reaction fit to a linear regression in Excel. Initial rates are extracted from the slope of the linear fit, $0.87 < R^2 < 0.99$. Concentration of TEMPO is varied from 5 – 45 mM and is indicated on each plot. Triplicate data sets for each concentration of TEMPO are presented.

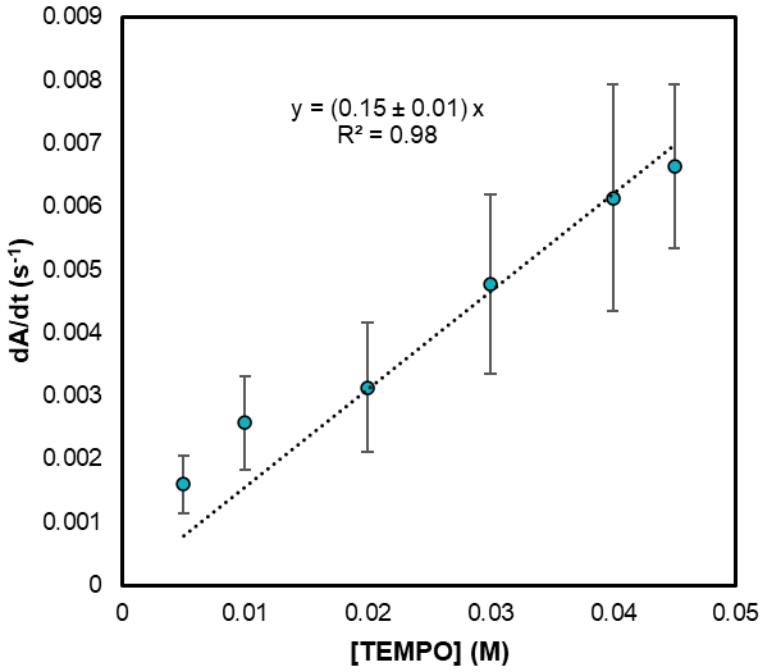

Figure S10. Plot of the initial rate *vs* the concentration of TEMPO, $k_{exp} = 0.15 \pm 0.01$ M^{-1} s^{-1} at 25 °C. k_{exp} is the experimentally derived rate constant obtained from the slope of the line. The normalized rate constant for number the number of H• transferred (k_{PCET}) can be obtained by diving k_{exp} by the number of reactive H on **2-$V_6O_6(OH_2)^{1-}$** such that: $k_{pcet} = k_{exp}/2 = 0.08$ M^{-1} s^{-1}.

.

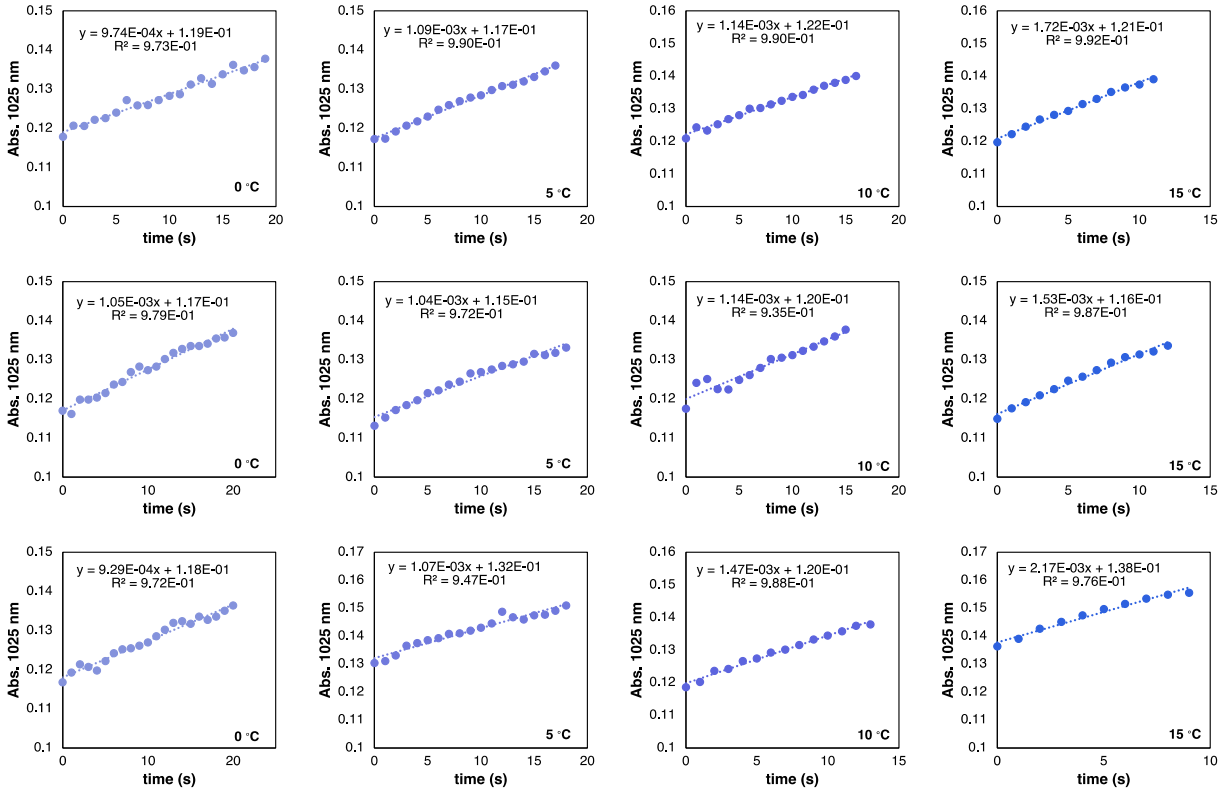

Figure S11. Kinetic traces at 1025 nm of 0.30 mM **2-$V_6O_6(OH_2)^{1-}$** + 10 mM TEMPO in THF, 0 – 15 °C. Traces are fit from 0 – 15 % completion of the reaction using a linear regression in Excel. Initial rates are extracted from the slope of the linear fit, $0.93 < R^2 < 0.99$. Triplicate data sets for temperature are presented.

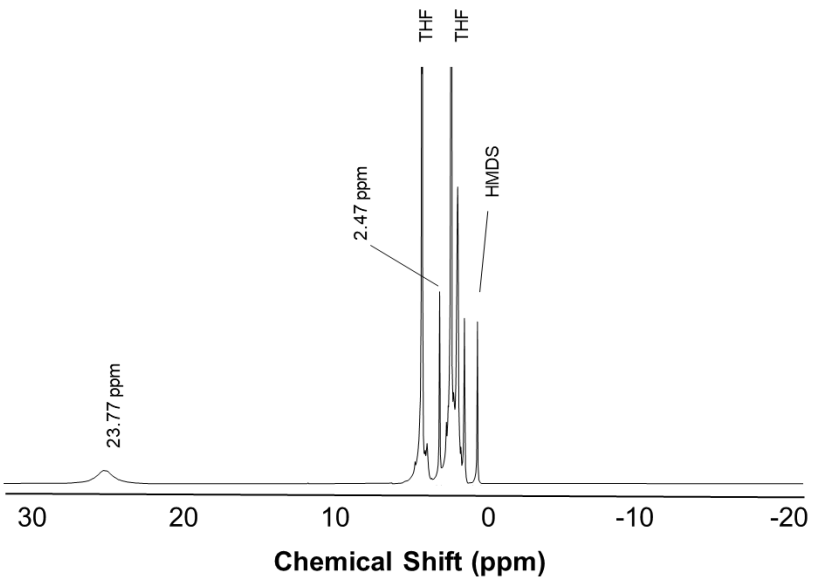

Figure S12. Exposure of 2.0 mM **2-$V_6O_6(OH_2)^{1-}$** to 1 atm of O_2 in THF-d_8 with hexamethyldisiloxane (HMDS) as an internal standard (1 mM) to show the formation of H_2O (2.47 ppm).

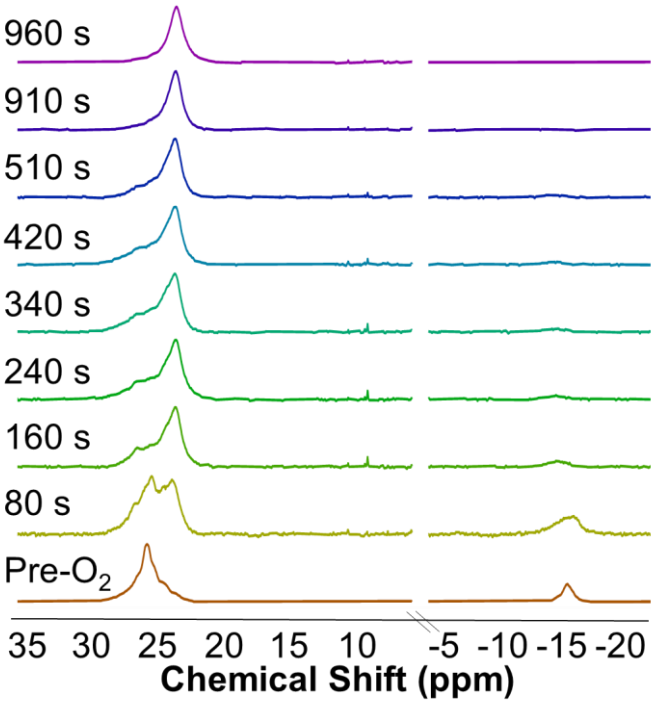

Figure S13. ^{1}H NMR of **2-$V_6O_6(OH_2)^{1-}$** + O_2 in THF-d_8 at room temperature, 21 °C.

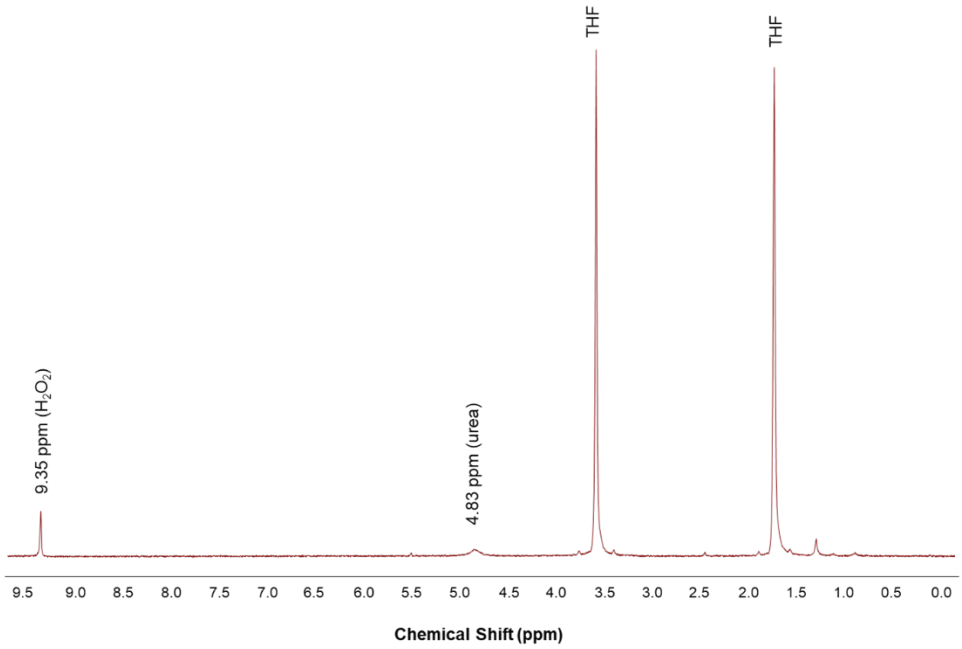

Figure S14. ^{1}H NMR of H_2O_2 urea in THF-d_8, 21 °C.

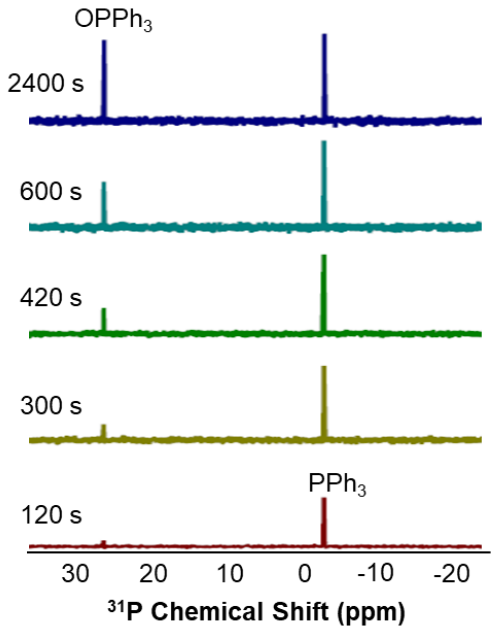

Figure S15. ^{31}P NMR of H_2O_2 urea adduct and PPh_3 in THF. Referenced to H_3PO_4, 21 °C. Control experiments reveal that PPh_3 is unreactive toward O_2, and previous work from our group has shown that **1-$V_6O_7^{1-}$** does not react with PPh_3 under the described reaction conditions, meaning any $OPPh_3$ formation is solely due to the presence of H_2O_2 produced *in situ*.[8]

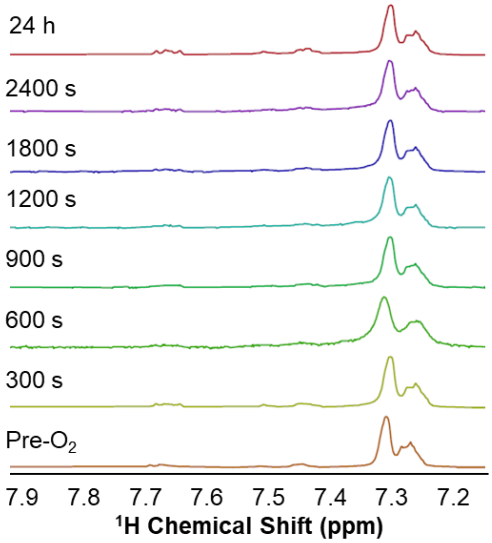

Figure S16. ^{1}H NMR of O_2 and PPh_3 in THF-d_8 at 21 °C, revealing only minor formation of $OPPh_3$ after 24 h of reaction time.

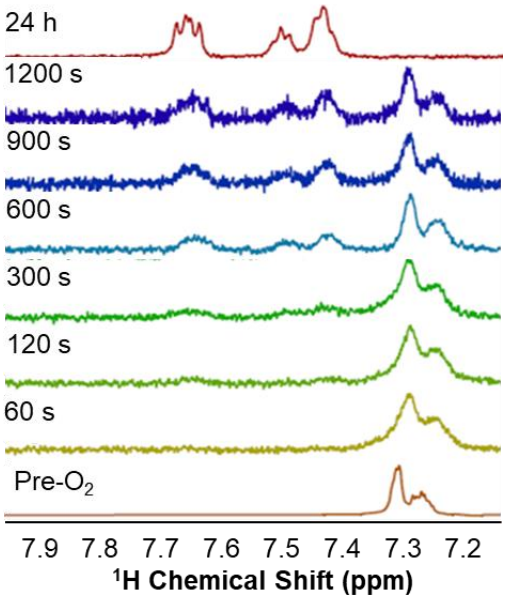

Figure S17. ^{1}H NMR of O_2, **2-$V_6O_6(OH_2)^{1-}$,** and PPh_3 in THF-d_8 at 21 °C. The observed qualitative conversion of PPh_3 to $OPPh_3$ is indicative of the formation of H_2O_2 *in situ*.

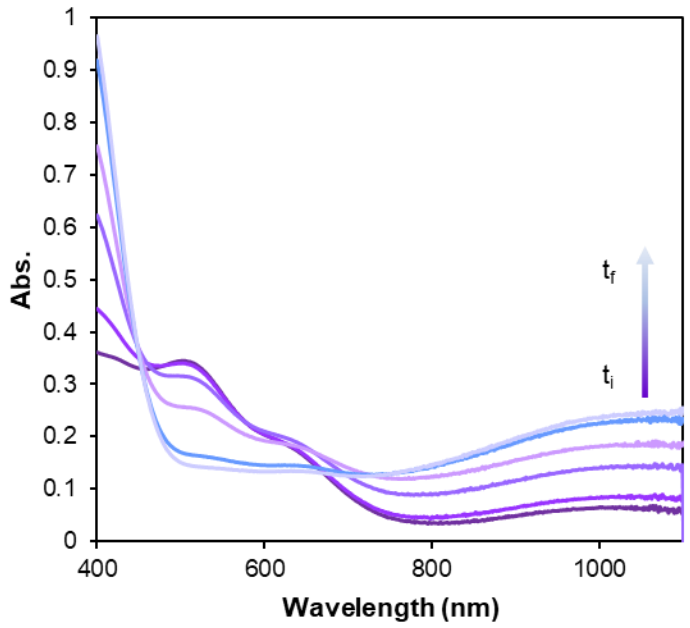

Figure S18. EAS Scanning kinetics of 0.30 mM **2-$V_6O_6(OH_2)^{1-}$** + 3 mM O_2 in THF. 25 °C. No obvious intermediate is formed unique of the products and reactants by EAS. t_f = ~ 3 hr.

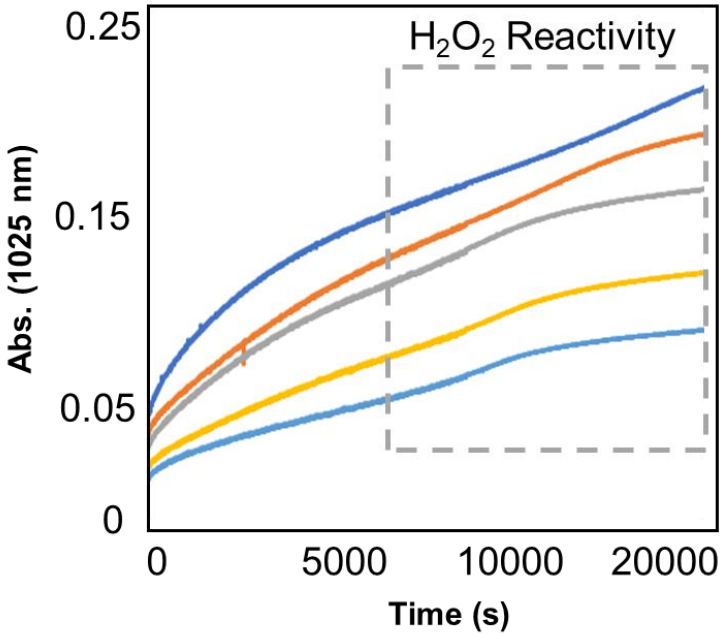

Figure S19. EAS Scanning kinetics at 1025 nm of varying concentrations of **2-$V_6O_6(OH_2)^{1-}$** (0.10 – 0.30 mM) + 3 mM O_2 in THF, 25 °C. As the H_2O_2 builds up in the reaction, it competes with the O_2 reduction causing the kinetic trace to deviate.

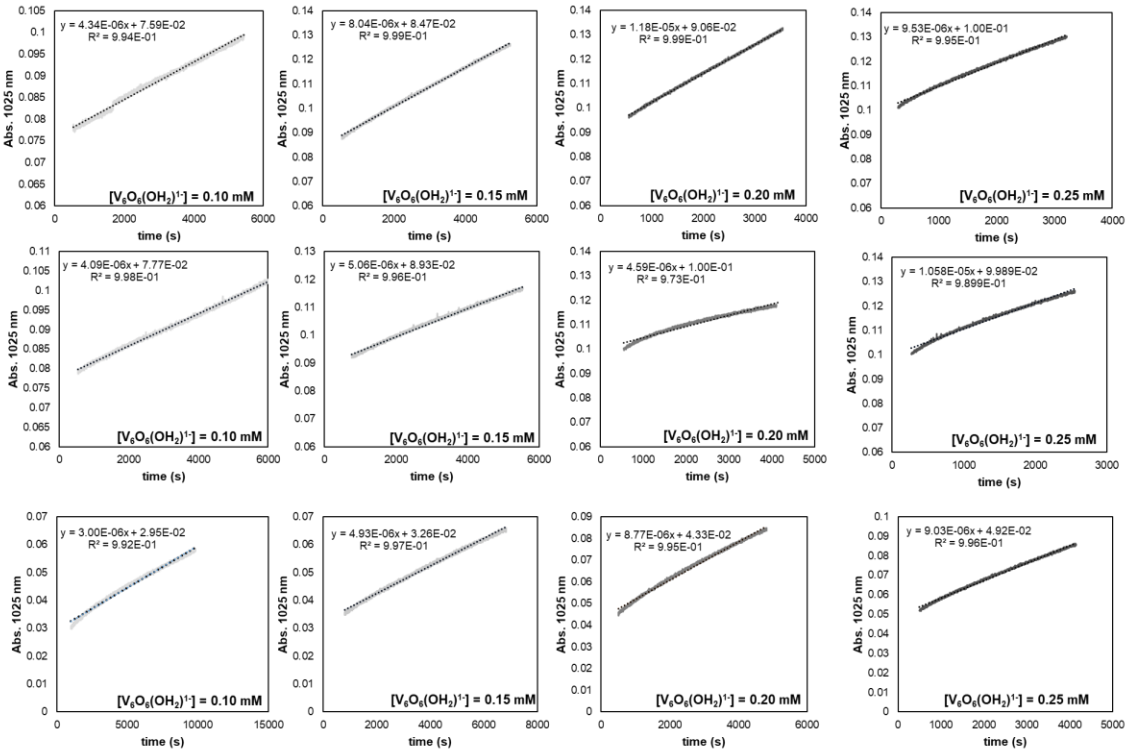

Figure S20. Kinetic traces at 1025 nm of varied concentration **2-$V_6O_6(OH_2)^{1-}$** + 3 mM O_2 in THF, 25 °C. Traces are fit from 5 – 15 % completion of the reaction using a linear regression in Excel. Initial rates are extracted from the slope of the linear fit, $0.97 < R^2 < 0.99$. Concentration of cluster is varied from 0.10 – 0.25 mM and is indicated on each plot. Triplicate data sets for each concentration of **2-$V_6O_6(OH_2)^{1-}$** are presented.

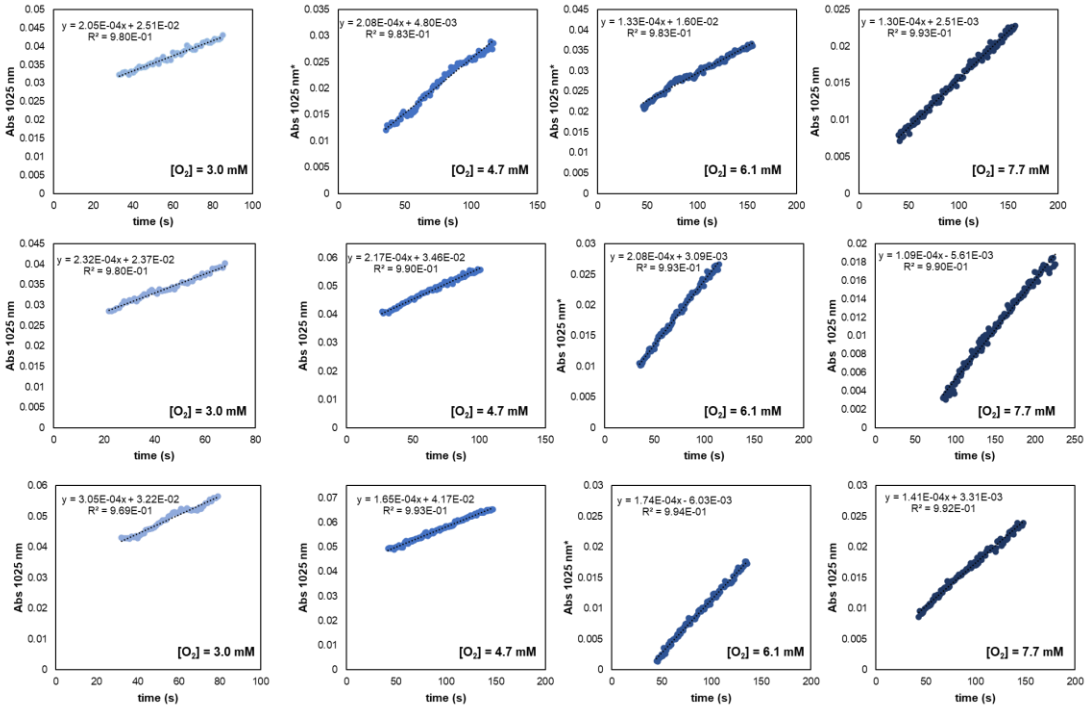

Figure S21. Kinetic traces at 1025 nm of 0.30 mM **2-$V_6O_6(OH_2)^{1-}$** + varied concentration of O_2 in THF, 25 °C. Traces are fit from 5 – 15 % completion of the reaction using a linear regression in Excel. Initial rates are extracted from the slope of the linear fit, $0.97 < R^2 < 0.99$. Concentration of O_2 is varied from 3.0 – 7.7 mM and is indicated on each plot. Triplicate data sets for each concentration of **2-$V_6O_6(OH_2)^{1-}$** are presented. *additional baseline correction is applied but ultimately has no effect on the initial rate.

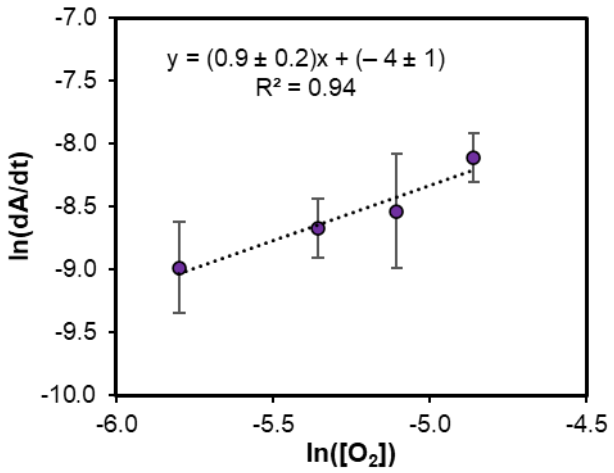

Figure S22. Log-log plot of the reaction of 0.3 mM **2-$V_6O_6(OH_2)^{1-}$** + XS O_2 in THF at 25 °C. Order with respect to O_2 is determined to be 0.9 ± 0.2 which is obtained from the slope of the line.

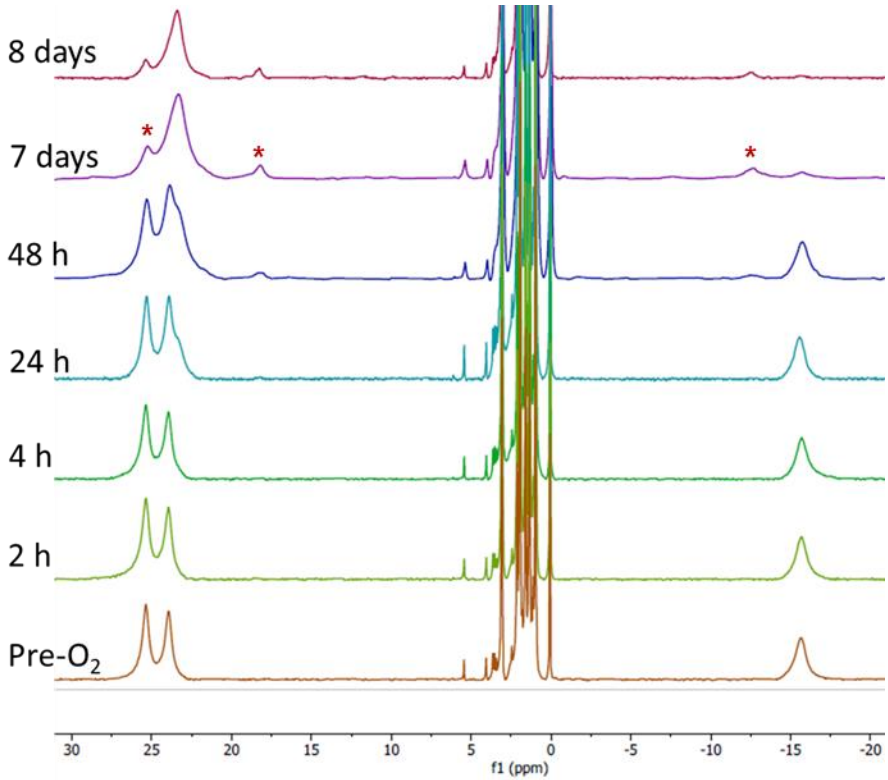

Figure S23. ^{1}H NMR of $V_6O_6(MeCN)(OMe)_{12}^{1-}$ in MeCN-d_3 + 1 atm of O_2 at 21 °C. The major product of the reaction is **1-$V_6O_7^{1-}$**; asterisks indicate the formation of $V_6O_6(MeCN)^0$, suggesting that oxidation of a minority of $V_6O_6(MeCN)^{1-}$ occurs *via* an ET in O_2.

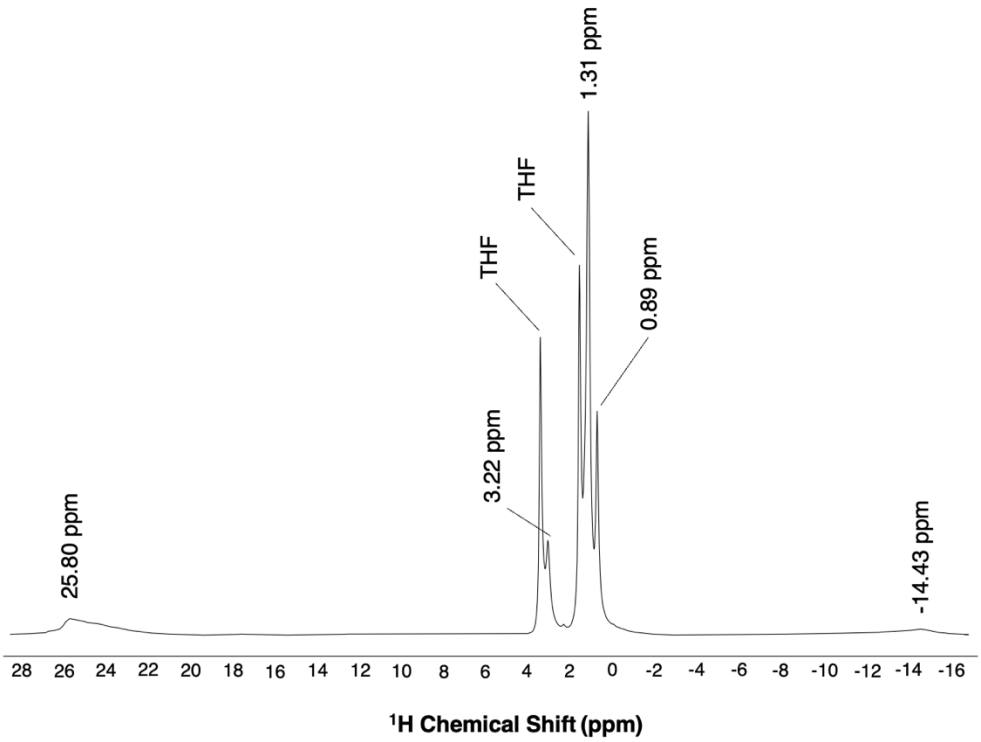

Figure S24. ^{1}H NMR of **2-$V_6O_6(OD_2)^{1-}$** in THF-d_8, 21 °C.

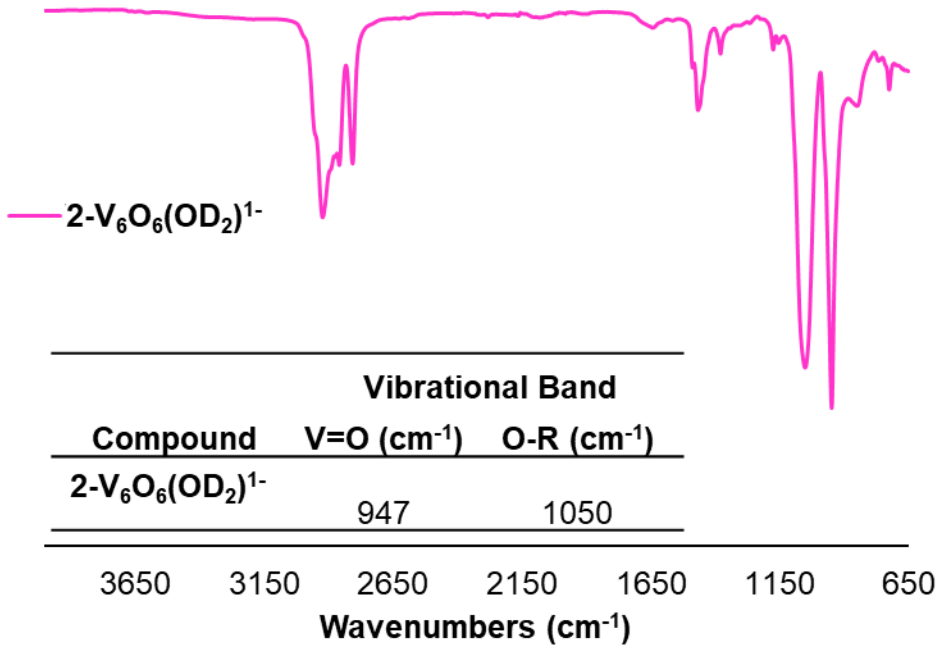

Figure S25. IR of **3-$V_6O_6(OD_2)^{1-}$**, neat 21 °C.

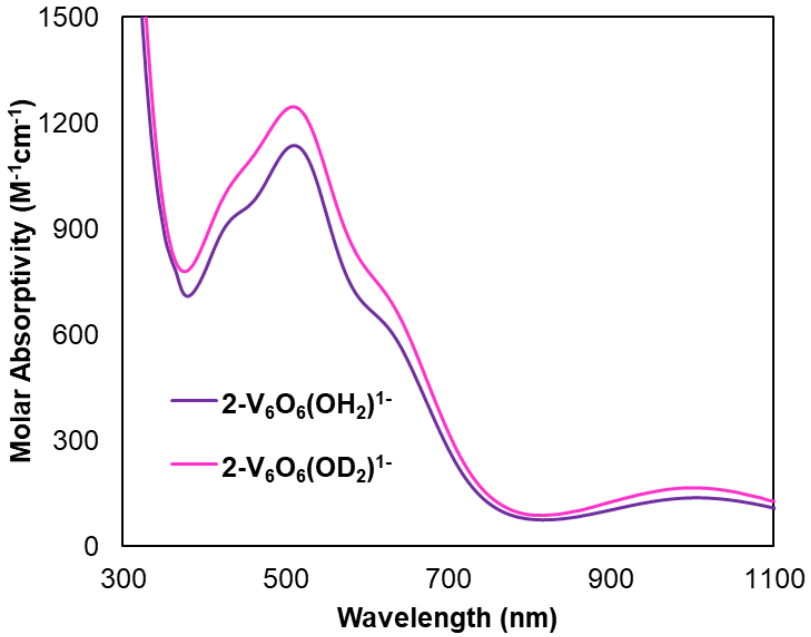

Figure S26. EAS of **2-$V_6O_6(OD_2)^{1-}$** (purple) and **2-$V_6O_6(OH_2)^{1-}$** (pink) in THF at 21 °C.

References.

1. C. Y. M. Peter, E. Schreiber, K. R. Proe and E. M. Matson, *Dalton Transactions*, 2023, **52**, 15775-15785.
2. J. Lee, K. Shizu, H. Tanaka, H. Nakanotani, T. Yasuda, H. Kaji and C. Adachi, *Journal of Materials Chemistry C*, 2015, **3**, 2175-2181.
3. E. Schreiber, A. A. Fertig, W. W. Brennessel and E. M. Matson, *Journal of the American Chemical Society*, 2022, **144**, 5029-5041.
4. R. E. H. Kuveke, L. Barwise, Y. van Ingen, K. Vashisth, N. Roberts, S. S. Chitnis, J. L. Dutton, C. D. Martin and R. L. Melen, *ACS Cent Sci*, 2022, **8**, 855-863.
5. J. Casado, M. A. Lopez-Quintela and F. M. Lorenzo-Barral, *Journal of Chemical Education*, 1986, **63**, 450.
6. H. C. Fry, D. V. Scaltrito, K. D. Karlin and G. J. Meyer, *Journal of the American Chemical Society*, 2003, **125**, 11866-11871.
7. R. G. Agarwal and J. M. Mayer, *Journal of the American Chemical Society*, 2022, **144**, 20699-20709.
8. B. E. Petel and E. M. Matson, *Chemical Communications*, 2020, **56**, 13477-13490.